# Chapter 5
# Sea Ice in a Climate Change Context

**Abstract** This chapter is a description of the role and importance of sea ice and sea ice biota on large scales and in relation to the effects of climate change. The decrease in summer sea ice extent and thickness are evident and described in (5.1). A Case Study 4 based on our observations in the Fram Strait and the Arctic Ocean illustrates some of the consequences and effects of increased inflow of warm Atlantic water (5.2). The question whether more light in an ice-free water column will increase pelagic primary production in the Arctic Ocean, is addressed with a model (5.3). Sea ice plays an important role in the exchange of $CO_2$ between ocean and atmosphere and the sea ice $CO_2$ pump is described in (5.4).

**Keywords** Effects of climate change · Ice extent · Atlantification · Primary production · $CO_2$

## 5.1 The Decrease in Arctic Sea Ice Extent and Thickness

Data on sea ice extent covering the entire Arctic Ocean first became available in 1979 when passive microwave remote sensing by satellites was developed (Wang and Overland 2009; Serreze et al. 2007). The Arctic sea ice extent varies annually between a maximum range of 14.3–16.3 million $km^2$ in March and a minimum range of 7.7–4.7 million $km^2$ in September, showing that about 8 million $km^2$ of sea ice melts every summer and develops again during autumn and winter. This is close to the area of Australia (7.7 million $km^2$). Figure 5.1a–b shows the maximum and minimum sea-ice extent on 18 March and 16 September 2012. The sea ice extent recorded in September 2012 was the lowest seasonal minimum extent ever recorded with satelites (Fig 5.1). Comparison of the September minimum sea ice extent and the bathymetry of the Arctic Ocean shows that it is the more shallow water (<200 m) shelf areas that are ice-free in summer. The large and extensive shelf areas are characteristic features of the Arctic Ocean where about half of the ocean seabed consists of shelf areas (Jakobsson 2016), potentially rich in oil and gas (Gautier et al. 2009). Sea ice extent varies annually and gradually between a maximum and minimum extent, as shown in a plot of year versus sea ice extent with maximum in March and minimum in September for the period 1979–2018 (Fig. 5.2a). Trend lines of annual maximum (March) and minimum (September) sea ice extent between 1979 and
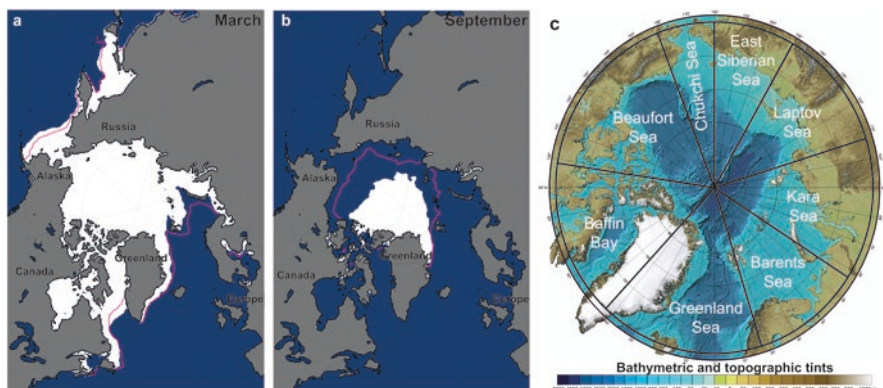
**Fig. 5.1** Sea ice extent on 18 March 2012 (**a**), and 16 September 2012 (**b**), where the magenta line is the median (1979–2000) sea ice extent (Courtesy: National Snow and Ice Data Center, Boulder, Colorado, USA http://nsidc.org/arcticseaicenews/2012/09/), and bathymetric map of the Arctic Ocean and the different sections referred to in the text (**c**)

2018 demonstrate a clear decrease during September of about 0.082 million km$^2$ per year or 3.2 million km$^2$ between 1979 and 2018 (Fig. 5.2b). The loss in March sea ice extent was half that, about 0.042 million km$^2$ per year equal to 1.6 million km$^2$, and demonstrates that the loss in sea ice extent is highest in September. The trend line for the September extent is: y = − 0.082 · x + 170.5 (Fig. 5.2a), which gives an ice-free Arctic Ocean in about 2080 if the decrease continues unabated. Longer time-series (1950–2015) from a high Arctic fjord, Young Sound in NE Greenland also show a significantly decreasing trend in the number of days with sea ice and thus, a corresponding longer open-water period is observed (Fig. 5.3). The loss in number of days with sea ice in this Young Sound area appears to be related to increased summer temperatures (Glud et al. 2007), which implies that the seasonal length of the ice–free period of this Arctic site has increased due to later freeze-up (Fig. 5.3). This also agrees with observations of later freeze-up from other Arctic sites (Parkinson 2014). A longer open-water period also results in an increasing potential for pelagic primary production, which agrees with estimates from remote sensing analysis of ocean colour that indicate a 30% increase in pelagic primary production between 1998–2009 in the Arctic Ocean (Arrigo and Dijken 2011). However, these trends vary between regions and the differences in increased pelagic production largely depend on the balance between the effects of sea ice decline, surface stratification, mixing and upwelling, and light conditions (Barber et al. 2015). Concomitant with a decrease in sea ice extent and ice cover duration in the Arctic, there has been a decrease in the thickness of the sea ice from an average of 3.5 m in November 1980 to about 2 m in November 2005 (Kwok and Rothrock 2009) and a parallel decrease in the age of the sea ice. The extent of multi-year ice defined as ice that survives one or more summer melts, was reduced by nearly 50% between 1999 and 2017 (Kwok 2018) with a decrease in coverage from about 22% in 1983 to about 5% in 2014 for multiyear ice >4 years. For multiyear ice >1 year
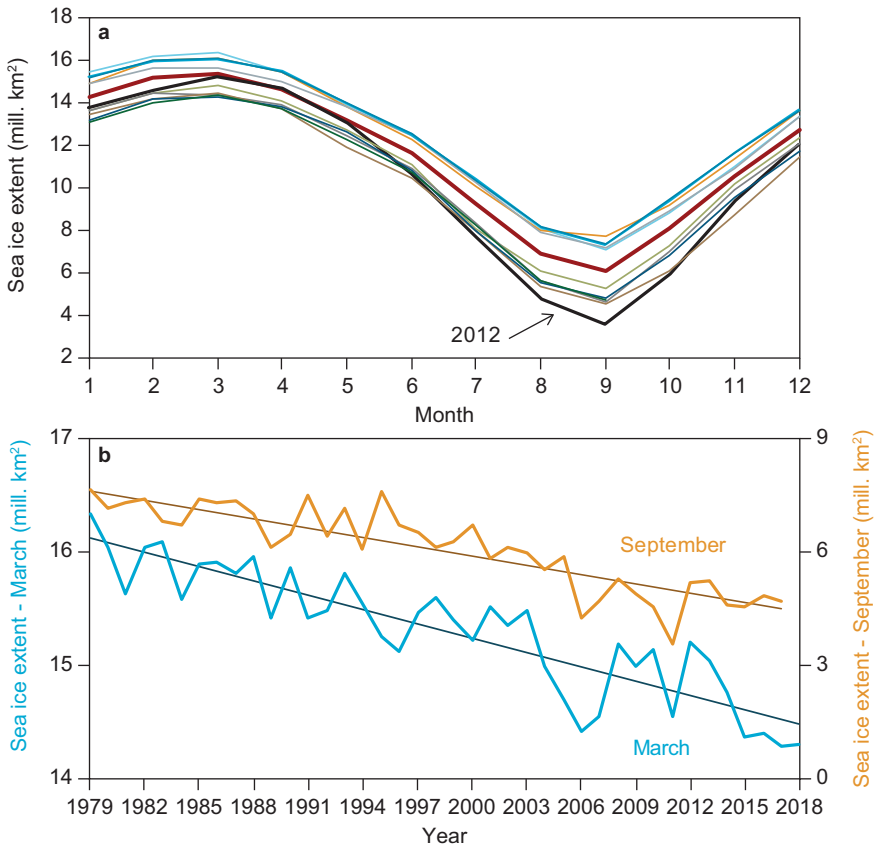
**Fig. 5.2** Annual variation between maximum sea ice extent in March and minimum in September comprising the period 1979–2018 where the year 2012 with the lowest minimum is marked, and bold red line represents the average for the period (**a**), and the minimum sea ice extent in September and maximum sea ice extent in March for each of the years 1979-2018 with trend lines. Note different ordinate scales for the maximum (blue) and minimum (orange) sea ice extent (**b**). (Data available at: https://nsidc.org/arcticseaicenews/sea-ice-tools/)

the coverage decreased from about 60% in 1983 to about 40% in 2014 (Fig. 5.4). The air temperature is increasing in the Arctic, and the increase is higher here than for the global average. The Arctic here refers to the area between latitudes 60 and 90°N, and the temperature anomaly, defined as the deviation from an average, is much higher in the Arctic than the global average (Fig. 5.5). The increase in air temperature reduces the growth of the sea ice, reinforcing the later autumn freeze-up, and enhances its melting. The significant decrease in summer sea ice extent and ice thickness are generally linked to the increase in air temperatures and secondly the increase in upper water column temperatures (Lindsay and Zhang 2005). There are, however, additional factors that also explain the decrease in summer sea ice extent. The lowest minimum extent observed until now was in September 2012
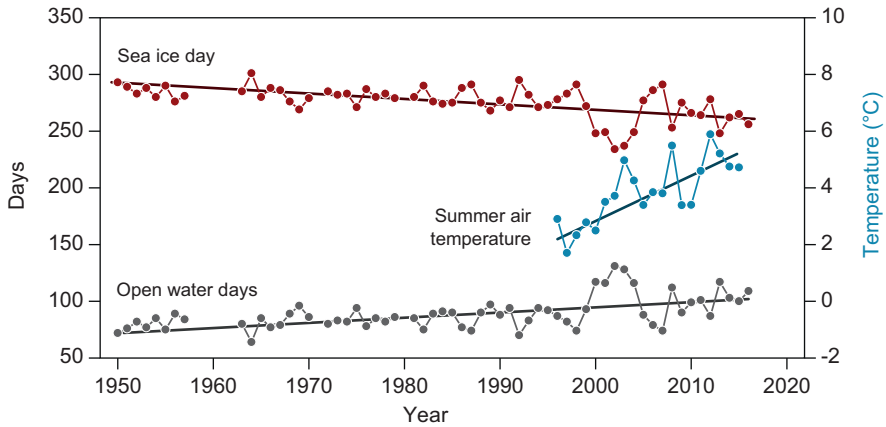
**Fig. 5.3**  The average sea ice days (red dots) and open water days (black dots) (1950-2015) and average summer air temperatures (blue dots) (1997-2015) in Young Sound, NW Greenland. (Modified from: Rysgaard and Glud 2007)
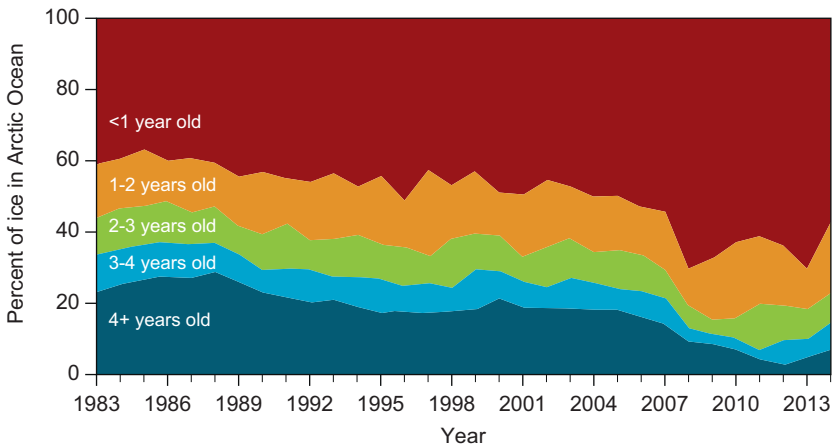


**Fig. 5.4**  The extent of sea ice as age groups: <1y, 1-2y, 2-3y, 3-4y, +4y at the end of summer between 1983 and 2014 in the Arctic Ocean. (Courtesy: Tschudi M. and Stewart S., University of Colorado, Boulder; Meiner W. and Stroeve J., NSIDC, http://nsidc.org/arcticseaicenews/2014/04/arctic-sea-ice-at-fifth-lowest-annual-maximum/)

(Fig. 5.2) and was related to extraordinary strong Arctic winds which transported large amounts of sea ice out of the Arctic Ocean through the Fram Strait (Zhang et al. 2013), eventually melting in the Fram Strait on its path south with the East Greenland current (Smedsrud et al. 2017). The general circulation of the Arctic Ocean comprises of a circular wind-driven current over the Canada Basin, termed the Beaufort Gyre, and a transpolar drift of ice and water from the Laptev and Kara Seas across the North Pole towards the Fram Strait (Fig. 5.6). The surface currents in the Arctic Ocean are colder and less saline, compared to the warm and saline
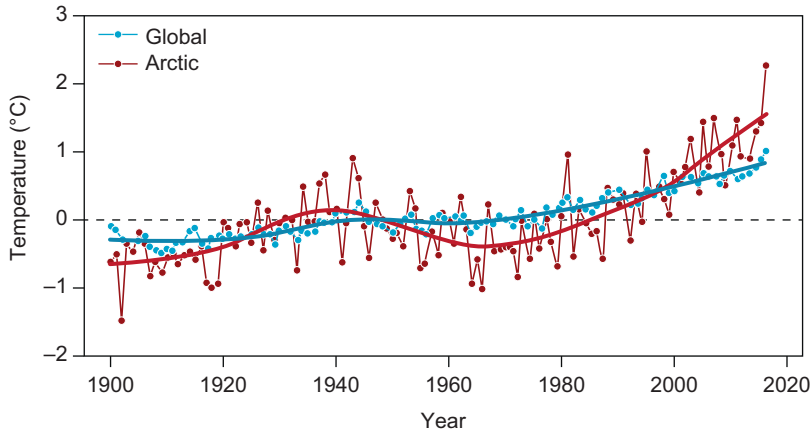
**Fig. 5.5** Annual temperature anomaly in the Arctic (red dots with thin line) and average (red solid line), annual temperature anomaly in global temperatures (blue dots with thin line), and average (blue solid line) between 1900 and 2017. Data available at https://data.giss.nasa.gov/gistemp/

Atlantic water that flows into the Arctic Ocean, where it sinks beneath the polar surface waters (Jakobsson et al. 2004) but is still a surface current in the Fram Strait. There has been an increase in the volume inflow of warm Atlantic water to the Arctic Ocean which is termed "Atlantification" (Polyakov et al. 2017; Randelhoff et al. 2016), and it was demonstrated that the increased inflow limits the southward expansion of winter sea ice in the Barents Sea (Barton et al. 2018). Larger areas in the Barents Sea are then ice-free during winter driven by the increased inflow of Atlantic water, and demonstrated by a comparison of March and median 1979–2000 sea ice extent where the Barents Sea winter ice edge has moved north-east (Fig. 5.1a). The water budget for the Arctic Ocean shows a discharge of warm saline Atlantic water into the Arctic Ocean and the pathways of colder, and less saline waters, which leave the Arctic Ocean through the Fram Strait, Narres Strait, and Canadian Archipelago (Fig. 5.6). It is also foreseen that precipitation and thus freshwater discharges into the Arctic Ocean will increase in the future (Carmack et al. 2015), which will enhance stratification of the water column and inhibit the vertical exchange of nutrients (Sect. 5.3).

## 5.2  A Glimpse into a Future Arctic Ocean - Case Study 4

The summer season offers research possibilities in the Arctic, as the thawing ice allows icebreakers access to areas that are largely inaccessible in winter. Here, two icebreaker cruises highlight the conditions and abiotic stressors that the sea ice community experiences during summer in the Fram Strait, and early autumn in the central Arctic Ocean.

**Fig. 5.6** Circulation and transport pathways of water masses in the Arctic Ocean, where red arrows signify warm and saline water from the Atlantic Ocean. This water sinks below the less saline surface waters influenced by freshwater outflow from large Russian rivers, and inflow through the Bering Strait. The Transpolar Drift (TD) transports ice and water from Laptev and Kara Sea towards the Fram Strait. *BC* Baffin Bay Current, *EGC* East Greenland current, *WGC* West Greenland Current, and *IrC* Irminger Current. (Modified from https://www.whoi.edu/main/topic/arctic-ocean-circulation)

### 5.2.1   *Melting Sea Ice in the Fram Strait*

Both the Fram Strait campaign and the Central Arctic Ocean campaign demonstrated the ecological consequences of melting of the sea ice and gave us a glimpse of what a future Arctic Ocean might look like. The purpose of the Fram Strait case study is also to highlight the strong west-east gradient (Randelhoff et al. 2018) in sea ice and ice algae conditions with the western section in the cold and low saline East Greenland Current, and eastern section in the warm saline Atlantic water (Fig. 5.6). As can be envisioned from the satellite image, there is a transport of ice out of the Arctic Ocean with the southward East Greenland current (Fig. 5.7). The annual amount of ice transported equals an area of about 500,000 km$^2$ and is
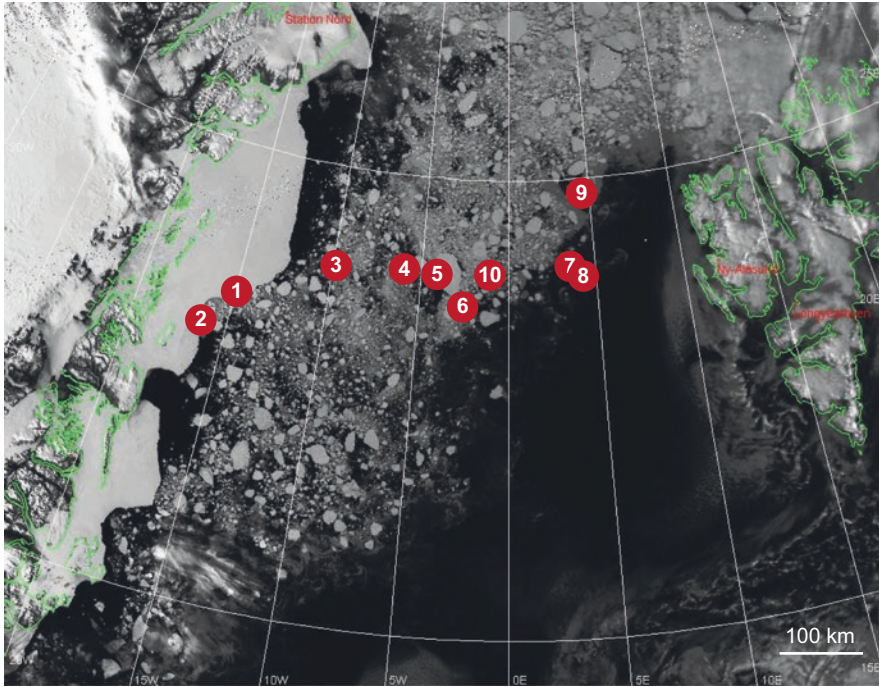
**Fig. 5.7** Satellite image of sea ice conditions in the Fram Strait on 10 June 2014 with drifting pack ice, large ice-floes and land-fast ice at the east Greenland coast. The numbers refer to station numbers in the Fram Strait sea ice campaign. (Courtesy: NOAA/National Oceanic and Atmospheric Administration)

equivalent to 10% of the summer sea ice in the Arctic Ocean (Comiso et al. 2008). We sampled a transect of stations between East Greenland and Svalbard in June 2014 with stations 1 and 2 at land-fast ice stations, meaning that the ice was fixed in position and attached to land (Fig. 5.7), and stations 3–10 in the pack ice, which is free-floating floes of different sizes from km to m (Figs. 5.7 and 5.11). The floes can be packed together due to wind and currents and large ridges can develop (Fig. 5.11), and the mixture of land-fast and pack-ice floes are clearly reflected in the different ice thicknesses (2.80–0.65 m) with thin ice stations to the east (Fig. 5.8a). Transmittance was high at the thinner ice at stations 7 and 8, and also low in Chl $a$, and lower (< 0.25) in maximum quantum yield ($F_v/F_m$) compared to western stations (~ 0.5) (Figs. 5.8b–c and 5.9). Ice algae at the bottom of the two stations had, in comparison, the highest concentrations of Diadinoxanthin and Diatoxanthin (Dtx + Ddx) relative to Chl $a$ at all stations. This demonstrates, that the ice algae at these stations started to adapt to the increased transmittance and higher light by developing sunscreen pigments (Dtx + Ddx) in the thinner ice as a response to melting from below in the warmer Atlantic water, with surface water temperatures of 1–2 °C compared to minus 1–2 °C at the western station 3 (Fig. 5.10b). With the increased inflow of warm Atlantic water (Polyakov et al. 2017) larger areas with ice in the Fram Strait would then be affected by warming and melting as observed here at stations 7 and 8, with significantly reduced ice algae biomass and low viability.
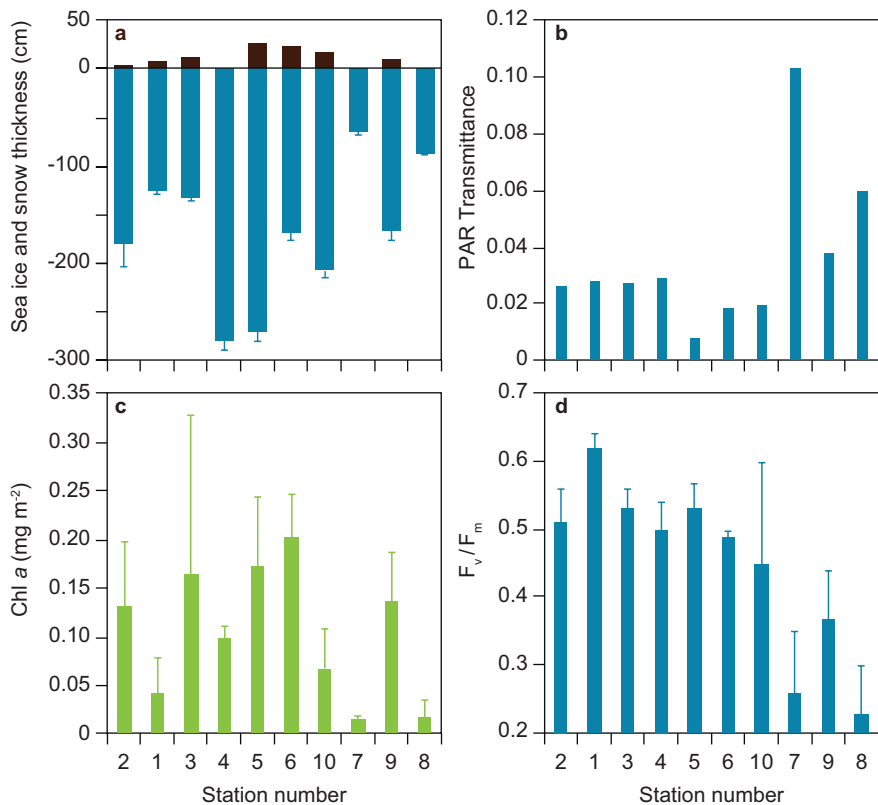
**Fig. 5.8** Snow thickness (black bars) and sea ice thickness (blue bars) (**a**), PAR transmittance (**b**), Chl *a* concentration (**c**), and maximum quantum yield ($F_v/F_m$) (**d**) at stations 1 to 10 in June 2014 in the Fram Strait. Values are means with standard deviations

**Fig. 5.9** Station 3 in the cold and low saline water originating from the Arctic Ocean and station 8 in the warm and high saline water flowing into the Arctic Ocean
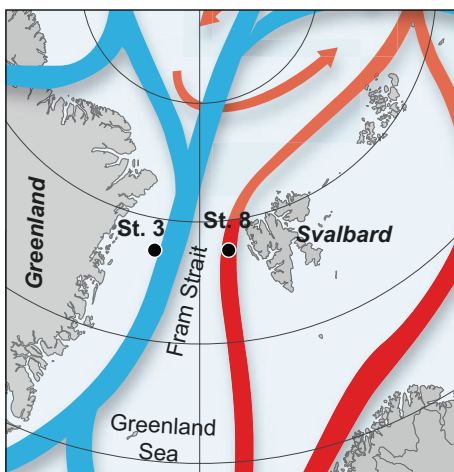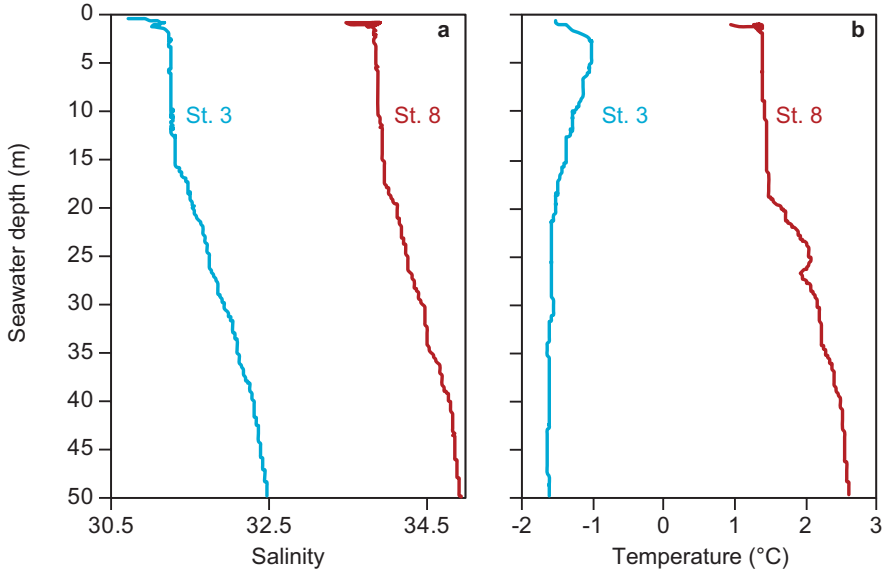
**Fig. 5.10**  Profiles of salinity (**a**), and temperature (**b**) with depth at stations 3 (blue line) and 8 (red line) in June 2014 in the Fram Strait

The west-east transect can be considered as a "space for time" concept where going from west to east (space) demonstrates the ecological consequences of melting of the sea ice with higher transmittances, and reduced biomass and viability. This will become the conditions at more sea ice sites in a future Arctic Ocean. Field work on the ice in the Fram Strait (Fig. 5.11).

### 5.2.2  Late and Future Arctic Ocean

There has been a gradual decrease in summer sea ice extent in the Arctic Ocean with a significant minimum in 2012 (Fig. 5.12a), where we participated in a research cruise in the Arctic Ocean on board the Swedish icebreaker *Oden*. A video shows *Oden* breaking heavy pack ice in the Amundsen Basin, Arctic Ocean. The purposes of this case study are to show and discuss the specific physiological conditions in the central of ice algae and related physical and optical properties at the end of summer in central Arctic Ocean. The ice algae was in very bad condition with low average maximum quantum yield *(F_v/F_m = 0.33)* (Fig. 5.13a), but what was to reason for this? Is transmittance increasing in a thinner ice and are the algae photo-damaged, and how low are nutrient conditions? Sampling was focused on the western part of the Amundsen Basin in central Arctic Ocean >86°N (Fig. 5.12), where station numbers are Julian day, i.e. station 226 was sampled on 13 August. Ice types were a mixture of first-year and multi-year ice with an average thickness of 152 cm (Fig. 5.13a), and identified based on bulk salinity of the ice.

**Fig. 5.11** Pressure ridges, sampling from ice floes and first-year ice, June 2014, Fram Strait. (Photographs by: Authors)

Lower salinities around 2–3 showed that the desalination processes of the ice had been active for a longer time period and indicative of a multi-year sea ice compared to first-year sea ice salinities around 5–7 (Warner et al. 2013; Lund-Hansen et al. 2015), and about 33% of the ice at stations were multi-year ice. Snow cover was absent in August/September, but transmittance in the ice was still comparatively low (0.05) (Fig. 5.13b), and with no difference in transmittance between first- or multi-year ice opposite to findings by Nicolaus et al. (2012). Ice algae occurred in very low (Chl $a$ < 0.05 mg m$^{-2}$) concentrations at most stations (Figs. 5.13c–d and 5.14) and were strongly dominated by diatoms (~80%) half of which was *Nitzschia frigida*, a very common Arctic diatom (Fig. 5.15a). Our August/September sampling was the end of season, and it is likely that ice algae were photodamaged after being exposed to 24 h of sunlight during summer months, but nutrient concentrations in the water were also low, e.g. nitrate (< 0.5 NO$_3^-$ µmol L$^{-1}$) (Fig. 5.15a), which might have affected conditions of the algae. Accordingly, a higher maximum quantum yield of the phytoplankton of 0.58 in the water below the ice compared to the ice algae (0.33) could reflect that phytoplankton is mixed up and down along light gradients and not fixed in position below the ice and exposed to perpetual light all through the summer. Ice thickness in the Arctic Ocean, north of Svalbard, has decreased about 0.5 m over the last 10 years (Kwok 2018) driven by the observed increase in Arctic air temperatures (Kurtz et al. 2014). A thinner ice with no snow cover will increase transmittance as observed in the Fram Strait which, in the future could have further negative consequences for the low light adapted ice algae in an environment of perpetual summer light as the Arctic Ocean.
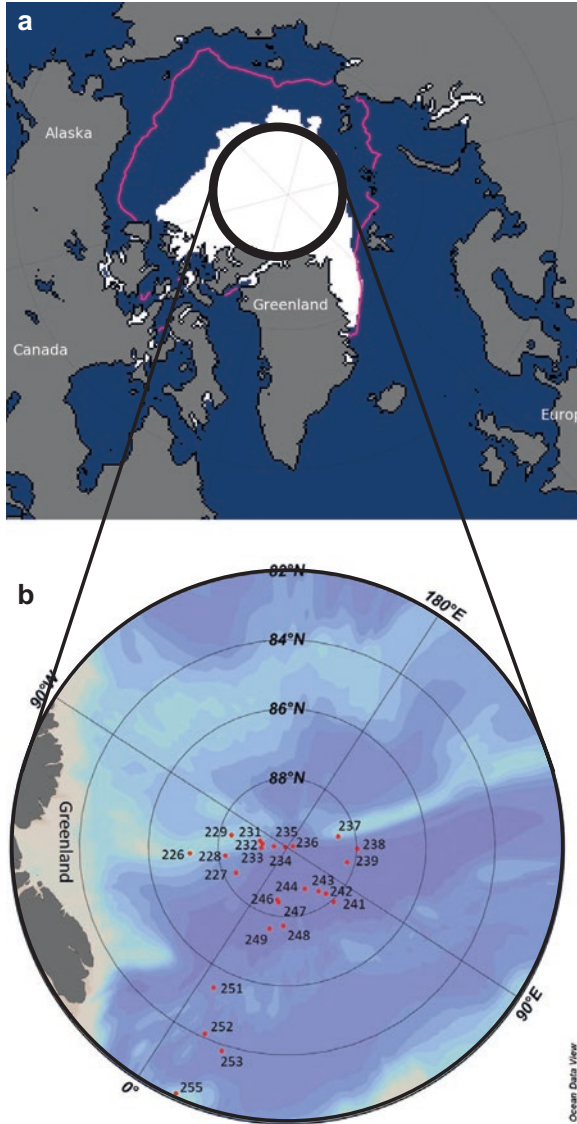
**Fig. 5.12** Sea ice extent on 16 September 2012 (**a**), where the magenta line is the median (1979-2000) sea ice extent. (Courtesy: National Snow and Ice Data Center, Boulder, Colorado, USA http://nsidc.org/arcticseaicenews/2012/09/), and bathymetric map of the Arctic Ocean with LOMROG III sea ice stations (**b**). (Modified from: Lund-Hansen et al. 2015)

## 5.3   Pelagic Primary Production Increase in Future Ice-Free Central Arctic Ocean?

Sea ice extent in the Arctic Ocean has decreased significantly during nearly four decades and is predicted to decrease as described above. The transition from a state with ice cover to a state of open water and its governing parameters is

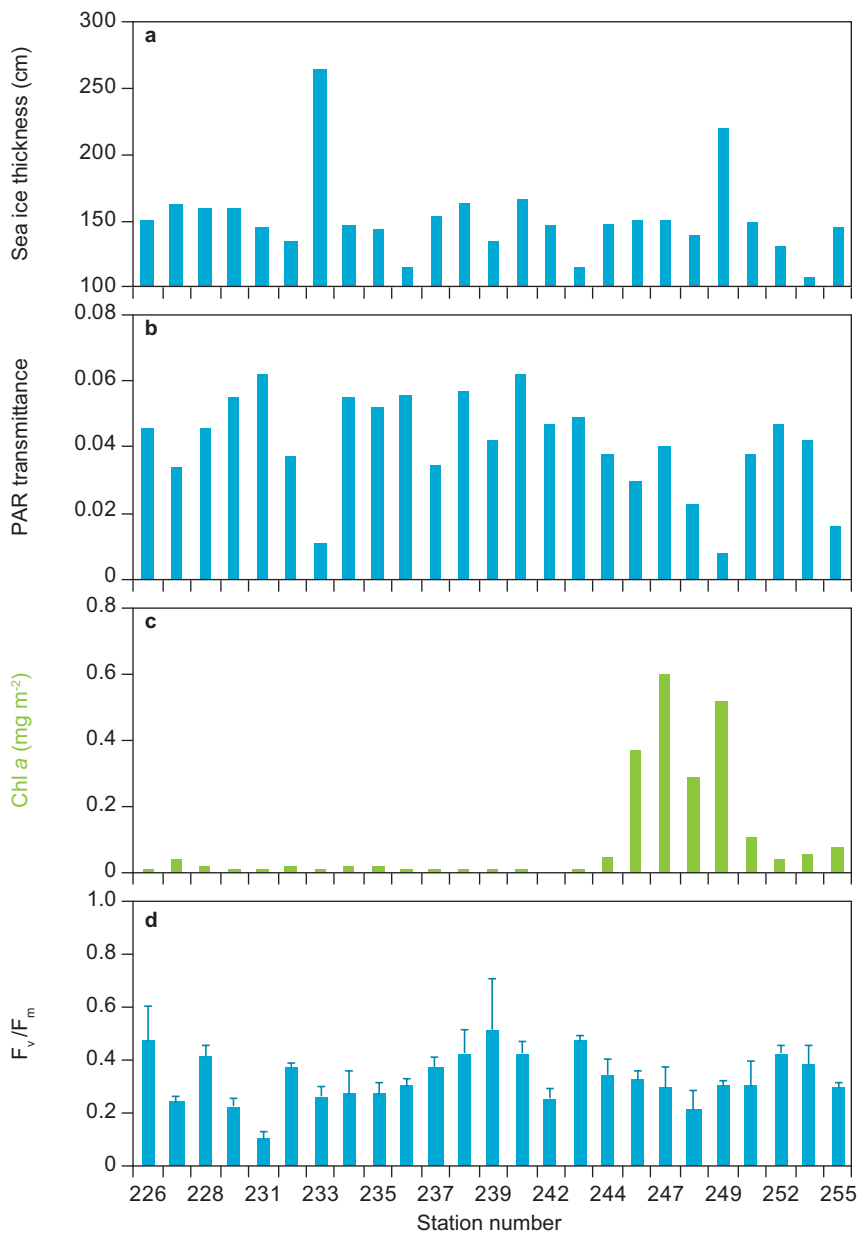**Fig. 5.13** Sea ice thickness (cm) (**a**), PAR transmittance (**b**), Chl *a* concentration (**c**), and maximum quantum yield ($F_v/F_m$) (**d**) at sea ice stations in August-September 2012, LOMROG III stations. Station numbers refer to Julian day. (Modified from: Lund-Hansen et al. 2015)

**Fig. 5.14** Maximum quantum yield ($F_v$ /$F_m$) in sea ice and seawater just below the ice, August-September 2012 at LOMROG III stations. (Modified from: Lund-Hansen et al. 2015)
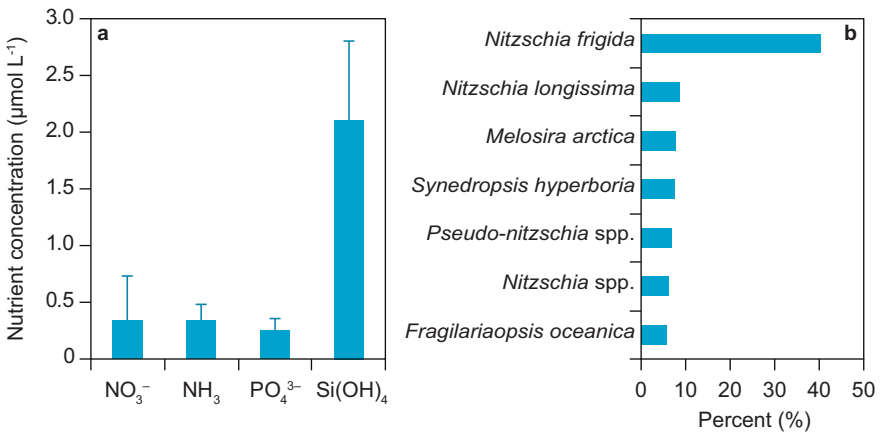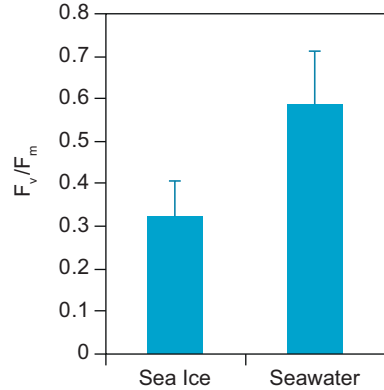




**Fig. 5.15** Average concentrations of nitrate, ammonium, phosphate and silicic acid in seawater just below ice (**a**), and abundances of dominant ice algae in ice bottom, August-September 2012, LOMROG III stations (**b**). (Modified from: Lund-Hansen et al. 2015)

conceptualized in Fig. 5.16. The ice-free water column will be exposed to winds and significantly higher irradiances with a water albedo of 0.1 compared to 0.6 for ice, and up to 0.8 if the ice is snow-covered. Wind exposure will induce mixing of the water column, whereby nutrients deeper in the water column can reach the surface and become available in the light-exposed surface waters. A question of high interest from a biological point of view is how the decrease in sea ice extent will affect the pelagic primary production in the Arctic Ocean? This is a question also of economic interest, as a higher primary production will result in higher secondary production and ultimately larger fish stocks and greater fisheries. Note that the conceptualization is simplified, as sea ice cover varies locally with larger and smaller leads (Fig. 5.17) (Assmy et al. 2017). Anyway, rates of primary production can be measured directly by applying the $^{14}$C method (Sect. 6.6), but satellite-based remote sensing techniques are often applied to estimate primary production rates for extensive areas that are difficult to access. Basically, the techniques rely on the
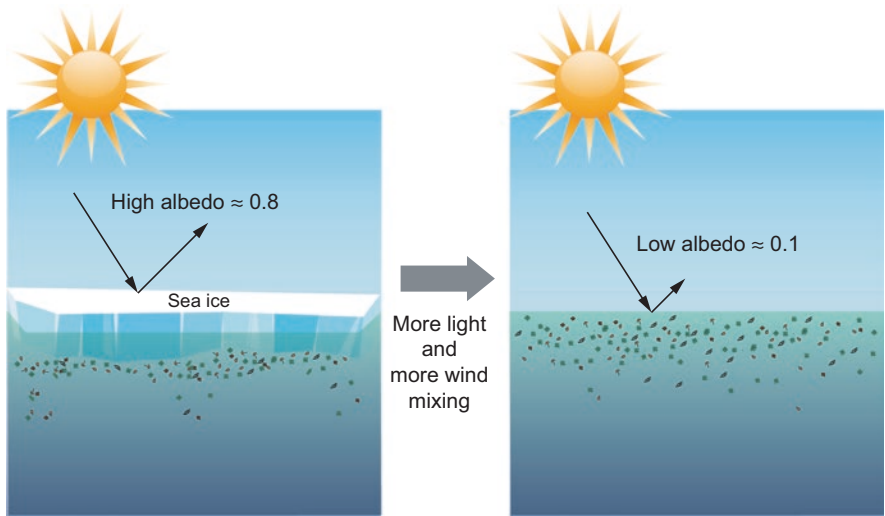
**Fig. 5.16** Change of Arctic Ocean marine conditions with and without a sea ice cover – increased light in the water column and increased wind mixing



**Fig. 5.17** Photo of sea ice, leads, and melt ponds near the North Pole, August 2012 from a helicopter. (Photograph by: Authors)
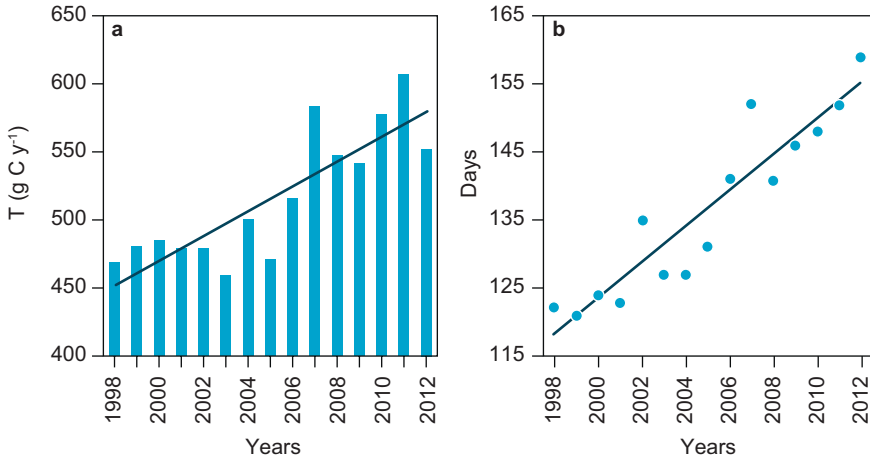
**Fig. 5.18** Annual net primary production (**a**), and length of open water period (**b**) between 1998 and 2012 in the Arctic Ocean. (Modified from: Arrigo and Dijken 2015)

assumption that a high Chl *a* concentration in the water presupposes a high primary production (Pabi et al. 2008). An equation is subsequently developed based on *in situ* measured primary production and Chl *a* concentrations, and the satellite-measured Chl *a* signal is then converted into a primary production (Arrigo et al. 2008; Arrigo and Dijken 2015). Application of this method has demonstrated that net primary production (NPP), i.e., gross primary production minus respiration, has increased significantly from 460 Tg C year$^{-1}$ to 560 Tg C year$^{-1}$ between 1998 and 2012 in the Arctic Ocean (Fig. 5.18a). Satellite-based primary production rates are then scaled up with the size of the area and production time, as for areas with several months in darkness. Apart from irradiance there are additional parameters that influence primary production such as nutrients, grazing, and stratification (Popova et al. 2012), but it appeared that a longer period of higher irradiance could explain the observed increases in NPP in the Arctic Ocean (Arrigo and Dijken 2015). The 21% increase in NPP correlates with a longer open water period, which has increased by more than a month from about 120 days (4 months) to 160 days (5.3 months) between 1998 and 2012 (Fig. 5.18b). The increase of about 100 Tg C year$^{-1}$ compares to the entire carbon production of the Barents Sea of 129 Tg C year$^{-1}$ in 2012 as the most productive shelf in the study (Arrigo and Dijken 2011). An average NPP increase of 21% conceals some significant regional differences between the shelves, ranging from 8.3% in Baffin Bay to 112.4% in the Laptev Sea. The Greenland Sea experienced, in comparison, a significant decrease in NPP (Arrigo and Dijken 2011), see Fig. 5.1c for locations. The study of Arrigo and Dijken (2015) was focused on the now summer ice-free shelf areas, but how will primary production change in the central Arctic Ocean when this area becomes ice-free in the near future (Fig. 5.2)? To answer the question we need a more detailed look of the Arctic Ocean. It is surrounded by large continents with limited exchange of water through

the Bering and Fram Straits, and the Barents Sea (Fig. 5.1). It receives a large and increasing amount of freshwater from Russian and Canadian rivers (Peterson et al. 2002), where the freshwater and melting of ice establish the surface Polar Mixed Layer, a cold (*ca.* -1.6 °C) and low saline (30–33) layer up to 40 m thick. A strong halocline separates the Polar Mixed Layer from the deeper lying warm and saline water of Atlantic origin (Fig. 5.19). The central Arctic Ocean is different to the shelves with deeper waters, generally low wind speeds due to the atmospheric high pressure covering the central Arctic (Overland et al. 2012), no supply of nutrients from surrounding rivers (Blais et al. 2017) and an extensive sea ice cover. Current primary production rates below the ice in the central Arctic Ocean in August–September are about 20 mg C m$^{-2}$ day$^{-1}$ (Fernández-Méndez et al. 2015), but will rates here increase with an ice-free water column and higher irradiances as observed on the shelf areas? In spite of low wind speeds there will be an increased mixing of the water column. But will the mixing bring nutrients to the sun-lit surface waters (Lincoln et al. 2016; Randelhoff et al. 2016) to fuel primary production? To address these questions in detail and more thoroughly, Lund-Hansen et al. (2019) applied a physical numerical 1-D model for the central Arctic Ocean with an added model describing primary production driven by wind speed, irradiance, nutrients, and Chl *a* concentrations as initial conditions. The model calculated primary production rates below the sea ice and for an ice-free period where the ice was removed in the



**Fig. 5.19** Vertical distribution of salinity (blue), Chl *a* (green), NO$_3$$^-$ (red), and PAR (red) below the ice in August 2012, Amundsen Basin, Arctic Ocean. (Modified from: Lund-Hansen et al. 2019)
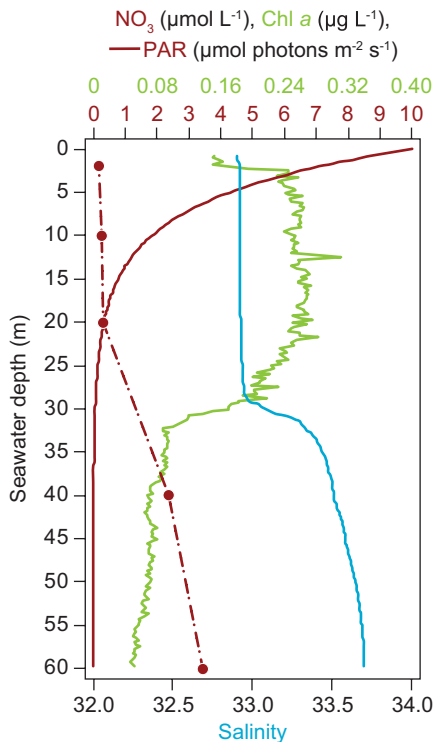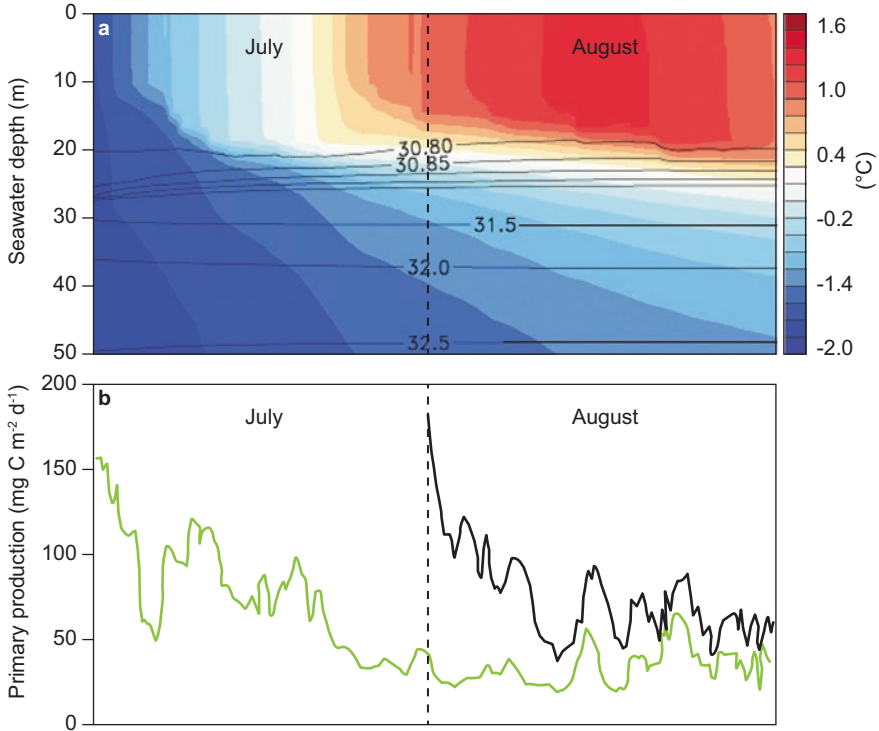
**Fig. 5.20** Model results with depth vs temperature for the water column (0-50 m), with isohalines (salinity) during ice-free July and August (**a**), and primary production during July and August (green line) and only August (black line) (**b**). (Modified from: Lund-Hansen et al. 2019)

model. A typical under-ice CTD profile near the North Pole shows a strongly stratified water column with a low (33) surface layer salinity, which increases to 33.7 at 60 m depth. Irradiance is low (10.0 μmol photons $m^{-2}$ $s^{-1}$) at the bottom of the ice, but there is still some (~0.3 μmol $L^{-1}$) nitrate ($NO_3$) in the surface layer where Chl *a* is also higher (0.24 mg Chl *a* $m^{-3}$) (Fig. 5.19). Primary production in the water column with ice was 3.9 mg C $m^{-2}$ $day^{-1}$. The surface layer is close to being depleted of nitrate and production is mainly sustained by regenerated nutrients in the surface layer. The limiting factor for the primary production is here nutrients, but mixing of the water was strongly limited by the ice, and transport of nutrients as nitrate towards the surface layer was low. Model results showed that the temperature of the surface water increased by 3–4 °C when ice-free and exposed to more light, but salinity stratification was still maintained (Fig. 5.20a). This implies that open water and wind mixing was too weak to fully break down stratification, but wind mixing events transported some nutrients to the surface waters, as shown by the peaks in primary production in early and late July (Lund-Hansen et al. 2019) (Fig. 5.20b). The model shows that primary production is initially high after the ice melts but decreases over time. Total integrated primary production reached 37.4 mg C $m^{-2}$

day$^{-1}$ in August and 55.2 mg C m$^{-2}$ day$^{-1}$ for July–August, which is higher, but still comparatively low. The 55.2 mg C m$^{-2}$ day$^{-1}$ equals 3.3 g C m$^{-2}$ year$^{-1}$ for a two-month period compared to the Barents Sea shelf production of 90 g C m$^{-2}$ year$^{-1}$ (Sakshaug 2004). The below-ice production of 3.9 mg C m$^{-2}$ day$^{-1}$ in the model is lower than the average 20.0 mg C m$^{-2}$ day$^{-1}$ measured in the same area (Fernandez-Méndez et al. 2015). However, productions of 37.4 mg C m$^{-2}$ day$^{-1}$ in August and 55.2 mg C m$^{-2}$ day$^{-1}$ for July-August are still higher. Primary production in the sea ice reached an average of 2.2 mg C m$^{-2}$ day$^{-1}$ in August–September (Fernández-Méndez et al. 2015), lower than the pelagic primary production. The model results demonstrate that an ice-free Arctic Ocean at latitudes >85°N will therefore not add significantly to overall Arctic marine primary production, predominantly due to the strong stratification of the water column. This stratification will only increase with higher precipitation and riverine discharges. The observed higher shelf production is because of a longer open water period at lower latitutes (Fig. 5.1), and therefore a stronger wind mixing in these areas transporting nutrients to the sun-lit surface waters (Randelhoff et al. 2016).

## 5.4   Sea Ice Driven $CO_2$ Uptake

This section briefly describes the drivers of inorganic carbon dynamics in sea ice and illustrates that sea ice can function as a $CO_2$ pump that draws $CO_2$ from the atmosphere into the ocean. The main driver of climate warming is the accumulation of $CO_2$ and other greenhouse gases in the atmosphere. The atmospheric concentration of $CO_2$ has increased from a preindustrial value of about 280 ppm to about 410 ppm (August 2019). Fortunately, the global oceans play an important role in buffering the effects of $CO_2$ emissions to the atmosphere by absorbing large amounts of the emitted $CO_2$ (approximately 30%; Sabine et al. 2012). Until recently, the role of sea ice-covered regions in ocean-atmosphere $CO_2$ exchange was assumed to be insignificant, because sea ice has been treated as an impermeable barrier to the exchange of $CO_2$ (Tison et al. 2002). However, scientists now know that sea ice can affect the capacity of the polar oceans for taking up atmospheric $CO_2$. One of the first descriptions of the transport of $CO_2$ across the sea ice-ocean interface (i.e., the sea ice $CO_2$ pump) was by Jones and Coote (1981). Now, 39 years later, understanding the seasonal events controlling the inorganic carbon dynamics, including both abiotic and biotic processes in sea ice-covered regions, is still a challenging subject. An important question to address within this field of research is: what is the relative impact of abiotic and biotic processes on carbon cycling in sea ice and what is the effect of these sea ice processes on the ocean carbon system? During winter, as sea ice grows, some of the salts and gases present in the seawater are rejected, whereas the rest are trapped within the brine pockets, channels and tubes (Petrich and Eicken 2017) (Fig. 5.21). A reduction in sea ice temperature decreases the brine volume (Fig. 5.22) with a concurrent increase in brine salinity and concentrations of solutes and gases in the brine (Cox and Weeks 1983; Papadimitriou et al. 2004). In addition,
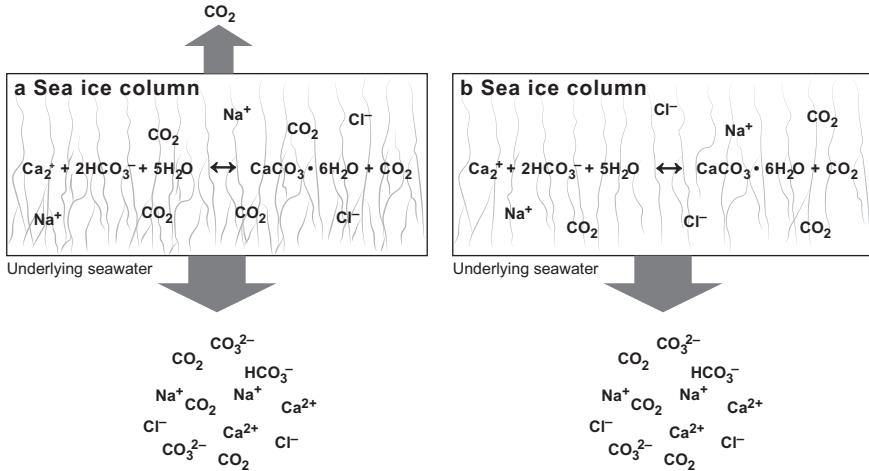
**Fig. 5.21** Conceptual model of the fate of $CO_2$ in growing permeable sea ice (**a**), and cold impermeable sea ice (**b**)

**Fig. 5.22** Thermal related evolution of the brine pore space as percent volume (P) at a set of temperatures (T). (Modified from: Pringle et al. 2009)
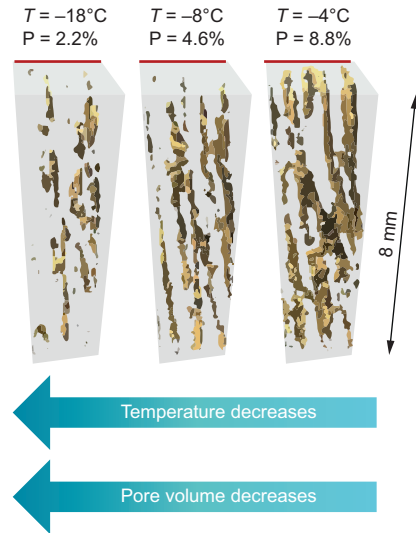


calcium carbonate ($CaCO_3$) can precipitate as brine temperatures decrease and solute concentrations increase. On the basis of thermodynamic equilibrium calculations, $CaCO_3$ precipitation was predicted to occur during natural sea ice formation (Assur 1960), which was later confirmed by observations: first in freezing seawater by Richardson (1976), then in artificial sea ice (Tison et al. 2002) and then finally observed in Antarctic and Arctic sea ice as ikaite crystals (Dieckmann et al. 2008, 2010). The precipitated ikaite crystals increase the amount of $CO_2$ in the brine beyond that attributed solely to the solubility effect. The ikaite crystals are trapped
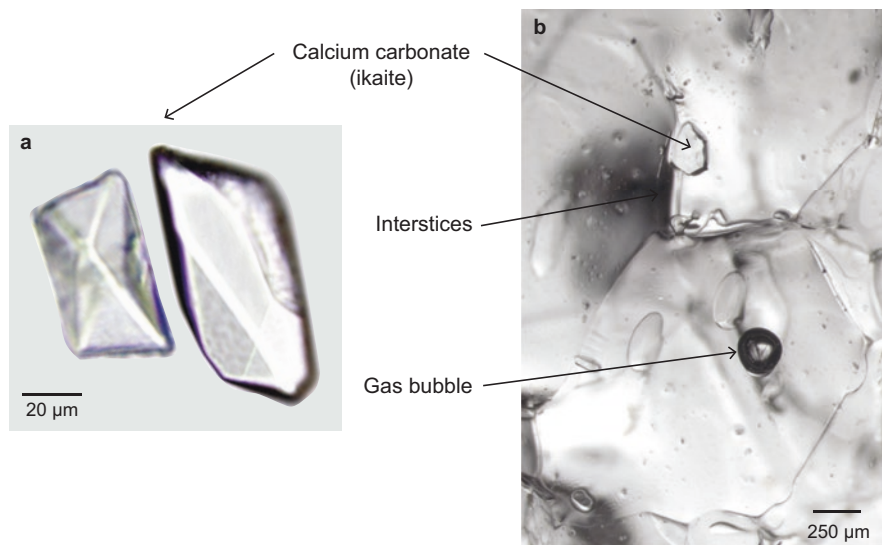
**Fig. 5.23** Microscopic image of ikaite crystals at high magnification (**a**), and microscopic image of sea ice showing ice crystal borders, brine pockets, air bubbles and ikaite crystals (**b**). (Modified from: Rysgaard et al. 2013)

within the interstices between the ice crystals (Rysgaard et al. 2013; Fig. 5.23), whereas the $CO_2$ released through the ikaite production within the brine can be lost from the sea ice to both the atmosphere and the underlying water (Fig. 5.21). However, when the sea ice temperature reaches $-5$ °C and the ice becomes less permeable for fluid transport, sea ice-air gas exchanges are also reduced, and $CO_2$ is mainly lost from the sea ice to the underlying water column (Fig. 5.21). Therefore, as sea ice grows, brine drainage can lead to an export of gases from the sea ice, leaving sea ice depleted in $CO_2$ compared to ambient seawater (Rysgaard et al. 2009). Brine drainage from sea ice causes the formation of cold, highly saline and dense water that sinks to deeper ocean layers. Observations in the Arctic also suggest that $CO_2$ by brine drainage can be transported below the pycnocline and, subsequently, be incorporated into intermediate and deep–water masses (Rysgaard et al. 2011). However, the fate of the rejected $CO_2$ in the water column is still poorly understood. Another important process during winter is the formation of frost flowers. As described in Sect. 2.5, frost flowers and brine skim can develop on the surface of newly formed mm-thick sea ice in cold air temperatures and at low wind speeds. Very high ikaite concentrations have been observed in this high-salinity brine skim and frost flowers within an hour of formation (Barber et al. 2014). Frost flowers are extremely effective collectors of drifting snow on sea ice and, with time, can be integrated into the snow layer on top of the sea ice. Recent studies have indicated that the incorporation of ikaite from frost flowers into the snow cover, together with the $CO_2$ that is released during ikaite precipitation, may result in snow-driven $CO_2$ outgassing under high wind speeds above winter sea ice (Sievers et al. 2015). The

overall outcome of this process is a closed $CO_2$ loop, with snow-driven $CO_2$ release above the ice in winter and $CO_2$ uptake during spring due to undersaturation in $CO_2$ after ikaite dissolution (Rysgaard et al. 2013; Søgaard et al. 2019). Due to their unique growth processes, chemical composition and later integration into the snow layer on top of sea ice, frost flowers and brine skim provide an important link for ocean-ice-atmosphere interactions in the Arctic. Furthermore, these cold and salty structures can support an ecosystem with millions of microbes inside (Barber et al. 2014). The question is: are the bacteria inside these structures active, and are cold-loving algae also living in frost flowers? What is the relative impact of these microbial processes on the net $CO_2$ exchange? All these questions remain unclear. However, the areal extent and periodicity of frost flowers and brine skim are expected to increase due to later autumn freeze-up, and a higher prevalence of thin and more fragile first-year sea ice with more leads where frost flowers can develop after refreezing (Isleifson et al. 2014). This will have significant implications for the $CO_2$ exchange and biogeochemical processes operating between the ocean-ice-atmosphere interfaces in the Arctic Ocean.

In spring, the warming of sea ice is accompanied by reduced ice salinity, approaching zero salinity, because of internal ice melt and brine flushing due to the brine draining of meltwater from surface melt ponds. As the sea ice warms, dissolution of ikaite (ikaite dissolves at temperatures above 4 °C), autotrophic assimilation of $CO_2$ through ice algal photosynthesis, and dilution of brine by melting sea ice are all processes that decrease the $pCO_2$ of the brines. At this point, the sea ice is depleted in $TCO_2$ and potentially enriched in TA due to dissolution of ikaite, which will result in a decrease in $pCO_2$ of the under-ice water (Else et al. 2011). Once the sea ice has melted totally, the surface seawater is highly undersaturated with $CO_2$, which will lead to an increase in the ocean uptake of atmospheric $CO_2$ (e.g. Miller et al. 2011). As mentioned above, microbial processes in sea ice can also change the $pCO_2$ of the brine and ultimately of the surface waters. In general, sea ice algae take up $CO_2$ and nutrients during the spring bloom, whereas sea ice bacteria may release $CO_2$ throughout the entire sea ice season. It is very important to understand the significance of these sympagic processes and their effects on net $CO_2$ exchange. However, few combined measurements of bacterial and primary productivity exist for Arctic sea ice, making it very difficult to assess the spatial and temporal impacts and effects of these processes (Fig. 5.24). Typically, the annual succession of the sea ice organisms seems to follow a distinctive pattern, with a winter stage characterized by a low but net heterotrophic activity (Fig. 5.25). This shift in the balance towards a net heterotrophic community is also consistent with the high concentrations of DOC and DON in sea ice, and the observed accumulation of macronutrients in winter sea ice (Fig. 4.3). Several studies have observed that DOM and EPS can be enriched in sea ice and that active phosphate (Helmke and Weyland 1995) and nitrogen (Baer et al. 2015) remineralization by sea ice bacteria actually occurs. The observed accumulation of algal nutrients indicates not only low ice algal productivity (allowing nutrients to accumulate) but also that heterotrophic bacteria are the main source of biogenic $CO_2$ in winter sea ice. The autotrophic activity exceeds the heterotrophic activity (Fig. 5.25) once light levels in the sea ice pass a critical level
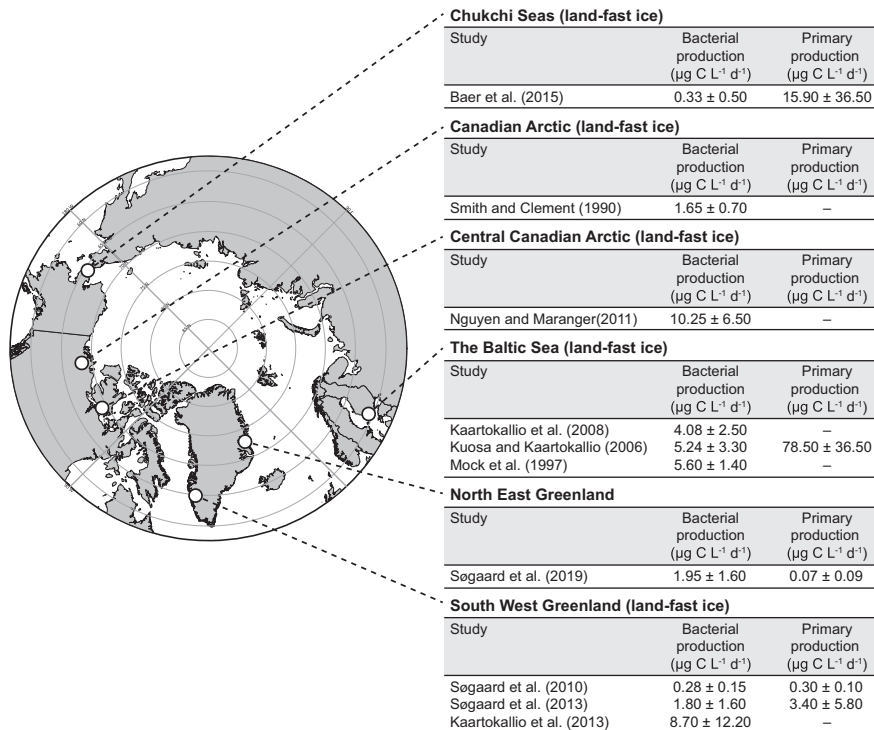
**Chukchi Seas (land-fast ice)**

| Study | Bacterial production (µg C L$^{-1}$ d$^{-1}$) | Primary production (µg C L$^{-1}$ d$^{-1}$) |
|---|---|---|
| Baer et al. (2015) | 0.33 ± 0.50 | 15.90 ± 36.50 |

**Canadian Arctic (land-fast ice)**

| Study | Bacterial production (µg C L$^{-1}$ d$^{-1}$) | Primary production (µg C L$^{-1}$ d$^{-1}$) |
|---|---|---|
| Smith and Clement (1990) | 1.65 ± 0.70 | – |

**Central Canadian Arctic (land-fast ice)**

| Study | Bacterial production (µg C L$^{-1}$ d$^{-1}$) | Primary production (µg C L$^{-1}$ d$^{-1}$) |
|---|---|---|
| Nguyen and Maranger(2011) | 10.25 ± 6.50 | – |

**The Baltic Sea (land-fast ice)**

| Study | Bacterial production (µg C L$^{-1}$ d$^{-1}$) | Primary production (µg C L$^{-1}$ d$^{-1}$) |
|---|---|---|
| Kaartokallio et al. (2008) | 4.08 ± 2.50 | – |
| Kuosa and Kaartokallio (2006) | 5.24 ± 3.30 | 78.50 ± 36.50 |
| Mock et al. (1997) | 5.60 ± 1.40 | – |

**North East Greenland**

| Study | Bacterial production (µg C L$^{-1}$ d$^{-1}$) | Primary production (µg C L$^{-1}$ d$^{-1}$) |
|---|---|---|
| Søgaard et al. (2019) | 1.95 ± 1.60 | 0.07 ± 0.09 |

**South West Greenland (land-fast ice)**

| Study | Bacterial production (µg C L$^{-1}$ d$^{-1}$) | Primary production (µg C L$^{-1}$ d$^{-1}$) |
|---|---|---|
| Søgaard et al. (2010) | 0.28 ± 0.15 | 0.30 ± 0.10 |
| Søgaard et al. (2013) | 1.80 ± 1.60 | 3.40 ± 5.80 |
| Kaartokallio et al. (2013) | 8.70 ± 12.20 | – |



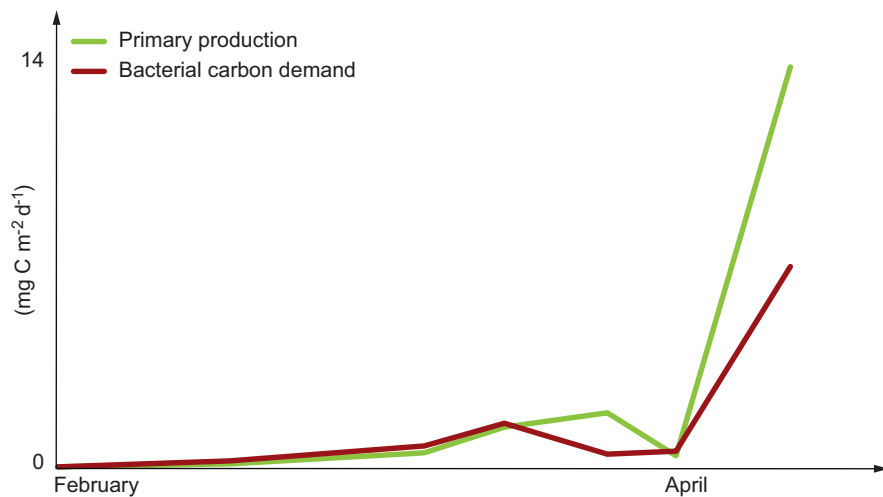**Fig. 5.24**  Sea ice bacterial and algal productivity compiled for different Arctic sea ice locations



**Fig. 5.25**  Bacterial carbon demand and primary production between February and April, SW Greenland. (Modified from: Søgaard et al. 2010)
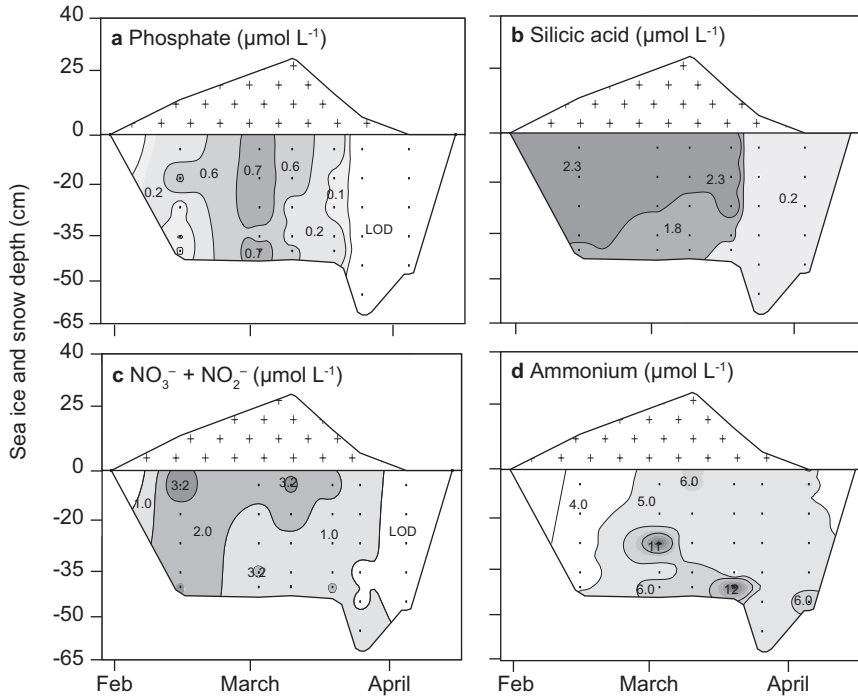
**Fig. 5.26** Seasonal development in Phosphate (**a**), silicic acid (**b**), nitrate and nitrite (**c**), and ammonium (**d**) concentrations in sea ice, in Malene Bight, SW Greenland. LOD is lower than detection limit. (Modified from: Søgaard et al. 2010)

(Fig. 1.1), resulting in rapid uptake of nutrients. A recent study has shown that the ice algal biomass was nutrient-limited in the late part of the sea ice season and that the nutrient concentrations in the ice fell to near zero, except ammonium concentrations that increased from winter to spring in the sea ice, indicating exchange and heterotrophic regeneration (Fig. 5.26) (Søgaard et al. 2010). Spring and summer is the season for increased ice algal activity, but even though the sea ice is net autotrophic, the ice bacterial activity is typically also highest in sea ice during spring and summer (Fig. 5.25). Although summer ice bacterial production rates are higher than reported winter rates, the bacterial production only represents 10% of primary production rates during summer. Therefore, at this spring/summer stage, the autotrophic assimilation of CO$_2$ depletes the $p$CO$_2$ but also the macronutrients of the brine.

One estimate indicates that the sea ice-driven CO$_2$ pump (i.e. including both abiotic and biotic processes in sea ice covered waters) is equivalent to 17–42% of the annual air-sea CO$_2$ flux in open ocean waters at high latitudes (Rysgaard et al. 2011). This estimate strongly contradicts the perception that sea ice acts only as a barrier, sealing off air-sea CO$_2$ fluxes in the Arctic Ocean, and emphasises that sea ice should be considered an essential part of the global carbon cycle. However, when considering the recent and ongoing changes in sea ice extent, age, thickness

and transmittance, a question arises: how will these changes affect the $CO_2$ uptake in a future Arctic Ocean? Recent estimates have ranged from a decrease to an increase in the net $CO_2$ uptake by the future Arctic Ocean (Mortenson et al. 2018). Therefore, there are still a lot of important future research questions to answer to better understand the importance of the sea ice driven $CO_2$ pump.

# References

Arrigo, K. R., Dijken, G. V., & Pabi, S. (2008). Impact of a shrinking Arctic ice cover on marine primary production. *Geophysical Research Letters, 35*, L19603. https://doi.org/10.1029/2008GL035028.

Arrigo, K. R., & Dijken, G. L. (2011). Secular trends in Arctic Ocean net primary production. *Journal of Geophysical Research, 116*. https://doi.org/10.1029/2011JC007151.

Arrigo, K. R., & Dijken, G. L. (2015). Continued increases in Arctic Ocean primary production. *Progress in Oceanography, 136*, 60–70. https://doi.org/10.1016/J.POCEAN.2015.05.002.

Assmy, P., Fernández-Méndez, M., Duarte, P., Meyer, A., Randelhoff, A., Mundy, C. J., Olsen, L. M., Kauko, H. M., Bailey, A., Chierici, M., Cohen, L., Doulgeris, A. P., Ehn, J. K., Fransson, A., Gerland, S., Hop, H., Hudsonm, S. R., Hughes, N., Itkin, P., Johnsen, G. M., King, J. A., Koch, B. P., Koening, Z., Kwaśniewski, S., Laney, S. R., Nicolaus, M., Pavlov, A. K., Polashenski, C. M., Provost, C., Rösel, A., Sandbu, M., Spreen, G., Smedsrud, L. H., Sundfjord, A., Taskjelle, T., Tatarek, A., Wiktor, J., & Wagner, P. M. (2017). Leads in Arctic pack ice enable early phytoplankton blooms below snow-covered sea ice. *Scientific Reports, 7*. https://doi.org/10.1038/srep40850.

Assur, A. (1960). *Composition of sea ice and its tensile strength*. U.S. Snow, Ice and Permafrost Establishment Research Report 44. https://hdl.handle.net/2027/uc1.31822020697603

Baer, S., Connelly, T. L., & Bronk, D. A. (2015). Nitrogen uptake dynamics in landfast sea ice of the Chukchi Sea. *Polar Biology, 38*, 781–797. https://doi.org/10.1007/s00300-014-1639-y.

Barber, D. G., Ehn, J. K., Pucko, M., Rysgaard, S., Deming, J. W., Bowman, J. S., Papakyriakou, T., Galley, R. J., & Søgaard, D. H. (2014). Frost flowers on young Arctic Sea ice: The climatic, chemical, and microbial significance of an emerging ice type. *Journal of Geophysical Research, Atmospheres, 119*, 11593–11612. https://doi.org/10.1002/2014JD021736.

Barber, D. G., Hop, H., Mundy, C. J., Else, B., Dmitrenko, I. A., Tremblay, J. E., Ehn, J. K., Assmy, P., Daase, M., Candlish, L. M., & Rysgaard, S. (2015). Selected physical, biological and biogeochemical implications of a rapidly changing Arctic Marginal Ice Zone. *Progress in Oceanography, 139*, 122–150. https://doi.org/10.1016/j.pocean.2015.09.003.

Barton, B., Lenn, Y.-D., & Lique, C. (2018). Observed atlantification of the Barents Sea causes the Polar front to limit the expansion of winter sea ice. *Journal of Physical Oceanography, 34*. https://doi.org/10.1175/JPO-D-18-0003.1.

Blais, M., Ardyna, M., Gosselin, M., Dumont, D., Bélanger, S., Tremblay, J. E., Gratton, Y., Marchesem, C., & Poulin, M. (2017). Contrasting interannual changes in phytoplankton productivity and community structure in the coastal Canadian Arctic Ocean. *Limnology and Oceanography, 62*, 2480–2497. https://doi.org/10.1002/lno.10581.

Carmack, E. C., Yamamoto-Kawai, M., Haine, T. W. N., Bacon, S., Bluhm, B. A., Lique, C., Melling, H., Polyakov, I. V., Straneo, F., Timmermans, M.-L., & Williams, W. J. (2015). Freshwater and its role in the Arctic marine system: Sources disposition, storage, export, and physical and biogeochemical consequences in the Arctic and global oceans. *Journal of Geophysical Research, 121*, 675–717. https://doi.org/10.1002/2015JG003140.

Comiso, J. C., Parkinson, C. L., Gersten, R., & Stock, L. (2008). Accelerated decline in the Arctic Sea ice cover. *Geophysical Research Letters, 35*, L01703. https://doi.org/10.1029/2007GL031972.

Cox, G. F. N., & Weeks, W. F. (1983). Equations for determining the gas and brine volumes in sea-ice samples. *Journal of Glaciology, 29*, 306–316. https://doi.org/10.3189/S0022143000008364.

Dieckmann, G. S., Nehrke, G., Papadimitriou, S., Göttlicher, J., Steininger, R., Kennedy, H., Wolf-Gladrow, D., & Thomas, D. N. (2008). Calcium carbonate as ikaite crystals in Antarctic Sea ice. *Geophysical Research Letters, 35*. https://doi.org/10.1029/2008GL033540.

Dieckmann, G. S., Nehrke, G., Uhlig, C., Göttlicher, J., Gerland, S., Granskog, M. A., & Thomas, D. N. (2010). Brief communication: Ikaite ($CaCO_3.6H_2O$) discovered in Arctic Sea ice. *The Cryosphere, 4*, 227–230. https://doi.org/10.5194/tc-4-227-2010.

Else, B. G. T., Papakyriakou, T. N., Galley, R. J., Drennan, W. M., Miller, A., & Thomas, H. (2011). Wintertime $CO_2$ fluxes in an Arctic polynya using eddy covariance**:** Evidence for enhanced air-sea gas transfer during ice formation. *Journal of Geophysical Research, 116*, C00G03. https://doi.org/10.1029/2010JC006760.

Fernández-Méndez, M., Katlein, C., Rabe, B., Nicolaus, M., Peeken, I., Bakker, K., Flores, H., & Boetius, A. (2015). Photosynthetic production in the Central Arctic Ocean during the record sea-ice minimum in 2012. *Biogeosciences, 12*, 3525–3549. https://doi.org/10.5194/bg-12-3525-2015.

Gautier, D. L., Bird, K. J., Charpentier, R. R., Grantz, H. D. W., Klett, T. R., Moore, T. E., Pitman, J. K., Schenk, C. J., Schuenemeyer, J. H., Sørensen, K., Tennyson, M. E., Valin, Z. C., & Wandreay, C. J. (2009). Assessment of undiscovered oil and and gas in the Arctic. *Science, 324*, 1175–1179. https://doi.org/10.1126/science.1169467.

Glud, R. N., Rysgaard, S., Kühl, M., & Hansen, J. W. (2007). The sea ice in young sound: Implications for carbon cycling. In S. Rysgaard & R. N. Glud (Eds.), *Carbon cycling in Arctic marine Ecosystems – Case study Young Sound* (Meddelelser om Grønland, Bioscience, Vol. 58) (pp. 62–85). Copenhagen: Copenhagen the Commission for Scientific Research in Greenland.

Helmke, E., & Weyland, H. (1995). Bacteria in sea ice and underlying water of the Eastern Weddell Sea in midwinter. *Marine Ecology Progress Series, 117*, 269–287.

Isleifson, D., Galley, R. J., Barber, D. G., Landy, J. C., Komarov, A. S., & Shafai, L. (2014). A study on the C-band polarimetric scattering and physical characteristics of frost flowers on experimental sea ice. *IEEE Transactions on Geoscience and Remote Sensing, 52*, 1787–1798. https://doi.org/10.1109/TGRS.2013.2255060.

Jakobsson, M., Grantz, A., Kristoffersen, Y., & Macnab, R. (2004). Bathymetry and physiography of the Arctic Ocean and its constituent seas. In R. Stein & R. W. MacDonald (Eds.), *The organic carbon cycle in the Arctic Ocean* (pp. 1–16). Berlin/Heidelberg/New York: Springer, 363 pp.

Jakobsson, M. (2016). Submarine glacial landform distribution in the Central Arctic Ocean shelf-slope-basin system. *Geological Society, London, Memoirs, 46*, 469–476. https://doi.org/10.1144/M46.179.

Jones, E. P., & Coote, E. R. (1981). Oceanic $CO_2$ produced by precipitation of $CaCO_3$ from brines in sea ice. *Journal of Geophysical Research, 86*, 11041–11043. https://doi.org/10.1029/JC086iC11p11041.

Kaartokallio, H., Tuomainen, J., Kuosa, H., Kuparinen, J., Martikainen, P. J., & Servomaa, K. (2008). Succession of sea-ice bacterial communities in the Baltic Sea fast ice. *Polar Biology, 31*, 783–793. https://doi.org/10.1007/s00300-008-0416-1.

Kaartokallio, H., Søgaard, D. H., Norman, L., Rysgaard, S., Tison, J.-L., Delille, B., & Thomas, D. N. (2013). Short-term variability in bacterial abundance, cell properties, and incorporation of leucine and thymidine in subarctic sea ice. *Aquatic Microbial Ecology, 71*, 57–73. https://doi.org/10.3354/ame01667.

Kuosa, H., & Kaartokallio, H. (2006). Experimental evidence on nutrient and substrate limitation of Baltic Sea sea-ice algae and bacteria. *Hydrobiologia, 554*, 1–10. https://doi.org/10.1007/s10750-005-1001-z.

Kurtz, N. T., Galin, N., & Studinger, M. (2014). An improved Cryosat-2 sea ice freeboard retrieval algorithm through the use of waveform fitting. *The Cryosphere, 8*, 1217–1237. https://doi.org/10.5194/tc-8-1217-2014.

Kwok, R., & Rothrock, D. A. (2009). Decline in Arctic Sea ice thickness from submarine and ICESat records: 1958-2008. *Geophysical Research Letters, 36*. https://doi.org/10.1029/2009GL039035.

Kwok, R. (2018). Arctic Sea ice thickness, volume, and multiyear ice coverage: Losses and coupled variability (1958–2018). *Environmental Research Letters, 13*, 105005. https://doi.org/10.1088/1748-9326/aae3ec.

Lincoln, B. J., Rippeth, T. P., Lenn, Y.-D., Timmermanns, M. L., Williams, W. J., & Bacon, S. (2016). Wind-driven mixing at intermediate depths in an ice-free Arctic Ocean. *Geophysical Research Letters, 43*, 9749–9756. https://doi.org/10.1002/2016GL070454.

Lindsay, R. W., & Zhang, J. (2005). Arctic Ocean ice thickness: Modes of variability and the best locations from which to monitor them. *Journal of Physical Oceanography, 36*, 496–506. https://doi.org/10.1175/JPO2861.1.

Lund-Hansen, L. C., Markager, S., Hancke, K., Stratmann, T., Rysgaard, S., Ramløv, H., & Sorell, B. (2015). Effects of sea-ice light attenuation and CDOM absorption in the water below the Eurasian sector of the Central Arctic Ocean. *Polar Research, 34*, 23978. https://doi.org/10.3402/polar.v34.23978.

Lund-Hansen, L.C., Bendtsen, J., Stratmann, T., Tonboe, R., Olsen, S., Markager, S. and Sorrell, B. (2019). Will primary production rates in the Amundsen Basin (Arctic Ocean) remain low in a future ice-free setting? *Journal of Marine Systems* (Accepted).

Miller, L. A., Papakyriakou, T. N., Collins, R. E., Deming, J. W., Ehn, J. K., Macdonald, R. W., Mucci, A., Owens, O., Raudsepp, M., & Sutherland, N. (2011). Carbon dynamics in sea ice: A winter flux time series. *Journal of Geophysical Research, 116*. https://doi.org/10.1029/2009JC006058.

Mock, T., Meiners, K. M., & Giesenhagen, H. C. (1997). Bacteria in sea ice and underlying brackish water at 54" 26' 50'' N (Baltic Sea, Kiel Bight). *Marine Ecology Progress Series, 158*, 23–40. https://doi.org/10.3354/meps158023.

Mortenson, E., Steiner, N., Monahan, A. H., Miller, L. A., Geilfus, N.-X., & Brown, K. (2018). A model-based analysis of physical and biogeochemical controls on carbon exchange in the upper water column, sea ice, and atmosphere in a seasonally ice-covered Arctic strait. *Journal of Geophysical Research: Oceans, 123*, 7529–7549. https://doi.org/10.1029/2018JC014376.

Nguyen, D. & Maranger, R. (2011) Respiration and bacterial carbon dynamics in Arctic sea ice. *Polar Biology, 34*, 1843–1855. https://doi.org/10.1007/s00300-011-1040-z.

Nicolaus, M., Katlein, C., Maslanik, J., & Hendricks, S. (2012). Changes in Arctic Sea ice result in increasing light transmittance and absorption. *Geophysical Research Letters, 39*. https://doi.org/10.1029/2012GL053738.

Overland, J. E., Francis, J. A., Hanna, E., & Wang, M. (2012). The recent shift in early summer Arctic atmospheric circulation. *Geophysical Research Letters, 39*. https://doi.org/10.1029/2012GL053268.

Pabi, S., Dijken, G. L., & Arrigo, K. R. (2008). Primary production in the Arctic Ocean, 1998–2006. *Geophysical Research Letters, 113*. https://doi.org/10.1029/2007JC004578.

Papadimitriou, S., Kennedy, H., Kattner, G., Dieckmann, G. S., & Thomas, D. N. (2004). Experimental evidence for carbonate precipitation and $CO_2$ degassing during sea ice formation. *Geochimica et Cosmochimica Acta, 68*, 1749–1761. https://doi.org/10.1016/j.gca.2003.07.004.

Parkinson, C. L. (2014). Spatially mapped reductions in the length of the Arctic Sea ice season. *Geophysical Research Letters, 41*, 4316–4322. https://doi.org/10.1002/2014GL060434.

Peterson, B. J., Holmes, R. N., McClelland, J. W., Vörösmarty, C. J., Lammers, R. B., Shiklomanov, A. I., Shiklomanov, I. A., & Rahmstorf, S. (2002). Increasing river discharge to the Arctic Ocean. *Science, 298*, 2171–2173. https://doi.org/10.1126/science.1077445.

Petrich, C., & Eicken, H. (2017). Overview of sea ice growth and properties. In D. N. Thomas (Ed.), *Sea Ice* (3rd ed., pp. 1–41). Chichester, 652 pp: Wiley Blackwell. https://doi.org/10.1002/9781118778371.ch1.

Popova, E. E., Yool, A., Coward, A. C., Dupont, F., Deal, C., Elliott, S., Hunke, E., Jin, M., Steele, M., & Zhang, J. (2012). What controls primary production in the Arctic Ocean? Results from an intercomparison of five general circulation models with biogeochemistry. *Journal of Geophysical Research, 117*. https://doi.org/10.1029/2011JC007112.

Polyakov, I. V., Pnyushkov, A. V., Alkire, M. B., Ashik, I. M., Baumann, T. M., Carmack, E. C., Goszczko, I., Guthrie, J., Ivanov, V. V., Kanzow, T., Krishfield, R., Kwok, R., Sundfjord, A., Morison, J., Rember, R., & Yulin, A. (2017). Greater role for Atlantic inflows on sea-ice loss in the Eurasian Basin of the Arctic Ocean. *Science, 356*, 285–291. https://doi.org/10.1126/science.aai8204.

Pringle, D. J., Miner, J. E., Eicken, H., & Golden, K. M. (2009). Pore space percolation in sea ice single crystals. *Journal of Geophysical Research, 114*, C12017. https://doi.org/10.1029/2008JC005145.

Randelhoff, A., Fer, I., Sundfjord, A., Tremblay, J.-É., & Reigstad, M. (2016). Vertical fluxes of nitrate in the seasonal nitracline of the Atlantic sector of the Arctic Ocean. *Journal of Geophysical Research, 121*, 5282–5295. https://doi.org/10.1002/2016JC011779.

Randelhoff, A., Reigstad, M., Chierici, M., Sundfjord, A., Ivanov, V., Cape, M., Vernet, M., Tremblay, J.-E., Bratbak, G., & Kristiansen, S. (2018). Seasonality of the physical and biogeochemical hydrography in the inflow to the Arctic Ocean through the Fram Strait. *Frontiers in Marine Science, 5*, 224. https://doi.org/10.3389/fmars.2018.00224.

Richardson, C. (1976). Phase relationships in sea ice as a function of temperature. *Journal of Glaciology, 17*, 507–519. https://doi.org/10.3189/S0022143000013770.

Rysgaard, S., & Glud, R. N. (Eds.). (2007). *Carbon cycling in Arctic marine ecosystems: Case study Young Sound* (Meddelelser om Grønland. Bioscience 58, 214 pp). Copenhagen: DCE.

Rysgaard, S., Bendtsen, J., Pedersen, L. T., Ramløv, H., & Glud, R. N. (2009). Increased $CO_2$ uptake due to sea ice growth and decay in the Nordic Seas. *Journal of Geophysical Research, 114*. https://doi.org/10.1029/2008JC005088.

Rysgaard, S., Bendtsen, J., Delille, B., Dieckmann, G. S., Glud, R. N., Kennedy, H., Mortensen, J., Papadimitriou, S., Thomas, D. N., & Tison, J.-L. (2011). Sea ice contribution to the air-sea $CO_2$ exchange in the Arctic and Southern Oceans. *Tellus B, 63*, 823–830. https://doi.org/10.1111/j.1600-0889.2011.00571.x.

Rysgaard, S., Glud, R. N., Lennert, K., Cooper, M., Halden, N., Leakey, R. J. G., Hawthorne, F. C., & Barber, D. (2012). Ikaite crystals in melting sea ice – Implications for $pCO_2$ and pH levels in Arctic surface waters. *The Cryosphere, 6*, 901–908. https://doi.org/10.5194/tc-6-901-2012.

Rysgaard, S., Søgaard, D. H., Cooper, M., Pućko, M., Lennert, K., Papakyriakou, T. N., Wang, F., Geilfus, N. X., Glud, R. N., Ehn, J., McGinnis, D. F., Attard, K., Sievers, J., Deming, J. W., & Barber, D. (2013). Ikaite crystal distribution in winter sea ice and implications for $CO_2$ system dynamics. *The Cryosphere, 7*, 707–718. https://doi.org/10.5194/tc-7-707-2013.

Sabine, C. L., Hankin, S., Koyuk, H., Bakker, D. C. E., Pfeil, B., Olsen, A., Metzl, N., Kozyr, A., Fassbender, A., Manke, A., Malczyk, J., Akl, J., Alin, S. R., Bellerby, R. G. J., Borges, A., Boutin, J., Brown, P. J., Cai, W. J., Chavez, F. P., Chen, A., Cosca, C., Feely, R. A., González-Dávila, M., Goyet, C., Hardman-Mountford, N., Heinze, C., Hoppema, M., Hunt, C. W., Hydes, D., Ishii, M., Johannessen, T., Key, R. M., Körtzinger, A., Landschützer, P., Lauvset, S. K., Lefèvre, N., Lenton, A., Lourantou, A., Merlivat, L., Midorikawa, T., Mintrop, L., Miyazaki, C., Murata, A., Nakadate, A., Nakano, Y., Nakaoka, S., Nojiri, Y., Omar, A. M., Padin, X. A., Park, G. H., Paterson, K., Perez, F. F., Pierrot, D., Poisson, A., Ríos, A. F., Salisbury, J., Santana-Casiano, J. M., Sarma, V. V. S. S., Schlitzer, R., Schneider, B., Schuster, U., Sieger, R., Skjelvan, I., Steinhoff, T., Suzuki, T., Takahashi, T., Tedesco, K., Telszewski, M., Thomas, H., Tilbrook, B., Vandemark, D., Veness, T., Watson, A. J., Weiss, R., Wong, C. S., & Yoshikawa-Inoue, H. (2012). Surface Ocean CO2 atlas (SOCAT) gridded data products. *Earth System Science Data Discussions, 5*, 781–804. https://doi.org/10.5194/essdd-5-781-2012.

Sakshaug, E. (2004). Primary and secondary production in the Arctic seas, 57-81. In R. Stein & R. W. MacDonald (Eds.), *The organic carbon cycle in the Arctic Ocean* (363 pp). Berlin/Heidelberg: Springer.

Serreze, M. C., Holland, M. M., & Stroeve, J. (2007). Perspectives on the Arctic's shrinking sea-ice cover. *Science, 315*, 1533–1536. https://doi.org/10.1126/science.1139426.

Sievers, J., Sørensen, L. L., Papakyriakou, T., Else, B., Sejr, M. K., Haubjerg Søgaard, D., Barber, D., & Rysgaard, S. (2015). Winter observations of $CO_2$ exchange between sea ice and the atmo-

sphere in a coastal fjord environment. *The Cryosphere, 9*, 1701–1713. https://doi.org/10.5194/tc-9-1701-2015.

Smedsrud, L. H., Halvorsen, M. H., Stroeve, J. C., Zhang, R., & Kloster, K. (2017). Fram Strait sea ice export variability and September Arctic Sea ice extent over the last 80 years. *The Cryosphere, 11*, 65–79. https://doi.org/10.5194/tc-11-65-2017.

Smith, R. E. H., & Clement, P. (1990). Heterotrophic activity and bacterial productivity in assemblages of microbes from sea ice in the high Arctic. *Polar Biology, 10*, 351–357. https://doi.org/10.1007/BF00237822.

Søgaard, D. H., Kristensen, M., Rysgaard, S., Glud, R. N., Hansen, P. J., & Hilligsøe, K. M. (2010). Autotrophic and heterotrophic activity in Arctic first-year sea ice: Seasonal study from Malene bight, SW Greenland. *Marine Ecology Progress Series, 419*, 31–45. https://doi.org/10.3354/meps08845.

Søgaard, D. H., Thomas, D. N., Rysgaard, S., Glud, R. N., Norman, L., Kaartokallio, H., Juul-Pedersen, T., & Geilfus, N.-X. (2013). The relative contributions of biological and abiotic process to carbon dynamics in subarctic sea ice. *Polar Biology, 36*, 1761–1777. https://doi.org/10.1007/s00300-013-1396-3.

Søgaard, D. H., Deming, J. W., Meire, L., & Rysgaard, S. (2019). Effects of microbial processes and $CaCO_3$ dynamics on inorganic carbon cycling in snow-covered Arctic winter sea ice. *Marine Ecology Progress Series*. https://doi.org/10.3354/meps12868.

Tison, J.-L., Haas, C., Gowing, M. M., & Sleewaegen, S. (2002). Tank study of physico-chemical controls on gas content and composition during growth of young sea ice. *Journal of Glaciology, 48*, 177–191. https://doi.org/10.3189/172756502781831377.

Wang, M., & Overland, J. E. (2009). A sea ice free summer Arctic within 30 years? *Geophysical Research Letters, 36*. https://doi.org/10.1029/2009GL037820.

Warner, K., Iacozza, J., Scharien, R., & Barber, D. (2013). On the classification of melt season first-year and multi-year sea ice in the Beaufort Sea using Radarsat-2 data. *International Journal of Remote Sensing, 34*, 3760–3774. https://doi.org/10.1080/01431161.2012.760855.

Zhang, J., Lindsay, R., Schweiger, A., & Steele, M. (2013). The impact of an intense summer cyclone on 2012 Arctic Sea ice retreat. *Geophysical Research Letters, 40*, 720–726. https://doi.org/10.1002/grl.50190.